.
2g-0160

# SEISMIC PERFORMANCE ASSESSMENT OF A MULTI-SPAN BRIDGE WITH ELASTOMERIC AND TRIPLE FRICTION PENDULUM BEARING

C. Trejo [1], C. Melchor [2], M. Torres [3]

[1] *Bachelor, Universidad Nacional de Ingeniería, ctrejor@uni.pe*
[2] *PhD Candidate, Imperial College London, c.melchor-placencia18@imperial.ac.uk*
[3] *Associate professor, Universidad Nacional de Ingeniería, mtorres@uni.edu.pe*

## *Abstract*

In the last decade, South America has experienced a substantial increase in the use of seismic isolation devices in bridge engineering projects. This increase could be explained as a result of the outstanding performance of seismically isolated bridges in the last two major earthquakes in the region: the Maule earthquake in 2010 (Chile) and the Muisne earthquake in 2016 (Ecuador). During these main seismic events, extensive damage and even collapse were observed in some non-isolated bridges, showing that these structures are still vulnerable to strong ground motions. Since the mid-2010s, key highway infrastructure has been built in high seismic hazard zones of Peru. A partial disruption of the functionality of these bridges during severe earthquakes could mean restricted access to emergency areas. Despite the reliability of seismic isolation techniques as a seismic hazard mitigation strategy, their use in key Peruvian bridges is still limited.

The aim of using seismic isolators is to shift the fundamental frequency of a structure away from the predominant energy-containing frequencies of an earthquake ground motion. As a result, reduced forces are transmitted to the substructure. Seismic isolators are also capable of providing energy dissipation with the aim of reducing the transmitted accelerations to the superstructure. The most common types of seismic isolators used in South America are elastomeric isolators and sliding isolators.

In this paper, elastomeric and sliding isolation techniques were applied to a critical non-isolated multi-span bridge with the aim of undertaking a deep comparative assessment of both isolation techniques. Triple Friction Pendulum Bearings (TFPB) and Lead Rubber Bearings (LRB) were selected as representative examples of elastomeric and sliding isolators, respectively. In the design of these isolation bearings, the values of isolated periods, post-yield stiffness and yield force of the TFPB system were set to be similar to that of the LRB system. This criterion was adopted for the purpose of comparing the unique effects of each type of isolator on the seismic response of the analyzed bridge. To perform the comparative assessment, a series of nonlinear dynamic analyses were carried out considering both horizontal components of seven seismic records. In the case of the LRB, a numerical model that considers the bidirectional response of the isolator was adopted. The strength degradation due to lead-core heating effects was also taken into account during the analysis. In the modeling of the TFPB, a series model that correctly describes each of the five stages of movement developed by this isolator and its bidirectional behavior was considered. To gain a fully comprehensive understanding of the behavior of these isolators, a series of benchmark tests were reproduced to validate the numerical models adopted. Upper and lower limit analyses were performed to identify the advantages and drawbacks of each isolation system. From the obtained results, it was found that the LRB system is capable of providing more uniform and lower seismic demands into the substructure; however, it induces greater isolator displacements in comparison with the TFPB system.

*Keywords: seismic isolation, seismic response, nonlinear dynamic analysis, bridge.*

## 1. Introduction

The concept of seismic isolation as a design strategy has been widely accepted in South America during the last decade due to the outstanding seismic performance of isolated structures in the last two major earthquakes occurred in the region. Since its beginning, these seismic protective devices have evolved over the years due to the technological advancements in the field. As a result of these developments, several types of seismic isolators have been used in bridges with the aim of providing lateral flexibility that shifts the period of the structure and reduces the seismic demands drastically. In addition, these devices are capable of dissipating energy and providing lateral resistance to service loads.

Currently, the most widely used isolators are being classified as elastomeric bearings and sliding bearings. Among these categories, Lead-Rubber Bearings (LRB) and Triple Friction Pendulum Bearings (TFPB) are the most representative.

Although both isolators have the same goal in common, the mechanism on how these devices work is unique and different from each other. The LRB isolator (Fig.1), consists of thin steel plates and rubber layers interconnected with a lead core in its centre. This core provides energy dissipation capacity as well as an initial stiffness to withstand the service loads [1]. The thin steel plates provide vertical stiffness to prevent the buckling of the rubber and also transmit the shear force to the lead core.

In contrast to LRB isolators, the TFPB isolators (Fig. 1) rely on their concave geometry and friction properties of their inner surfaces. Isolated structures with these seismic devices experience a pendulum movement, as the isolator slider moves over the concave plate. During this movement, energy dissipation is produced due to the friction between the sliding surfaces. The dynamic characteristics of these types of isolators are a function of the supported mass, the properties of the sliding surface and the concave radius of the plate [1].
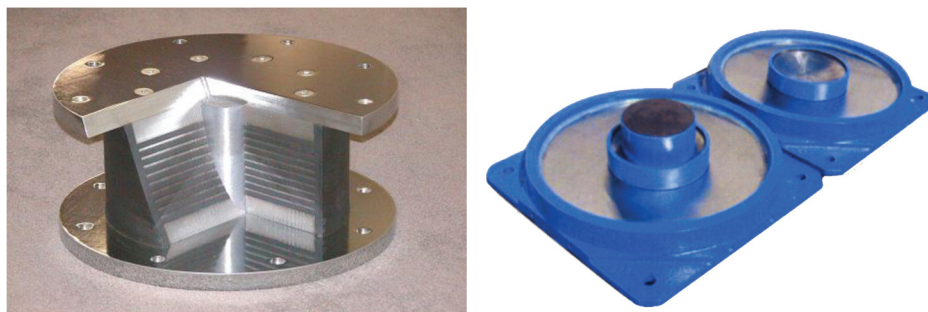


Fig. 1 – Lead rubber bearing (LRB) and Triple Friction Pendulum Bearings (TFPB)

This article presents a comparative assessment of the seismic performance of an isolated bridge with LRB and TFPB isolators. In the first stage of this work, the hysteric behaviour of these seismic protective devices was studied replicating the results obtained in previous benchmark test in order to gain a comprehensive understanding of their behaviour. Subsequently, the seismic response of an isolated three-span continuous using LRBs and TFPBs was assessed. For this purpose, a separate design of both isolators was carried out adopting the criteria established by Eröz and DesRoches [2], in which one criterion states that the obtained periods must be similar. In the estimation of seismic responses, a series of time history analyses were performed considering seven seismic records. In the isolated bridges the maximum distortions in the columns ($d_{max}$), the maximum isolator forces (MIF) and the maximum isolator displacements (MID) were compared.

## 2. Hysteretic models

Most of the numerical models implemented to describe the hysteretic behaviour of elastomeric and sliding isolators are mainly based on the hysteretic model developed by Wen [3]. In the particular case of LRBs, its bi-directional hysteretic behaviour is described through the following equation

$$\begin{Bmatrix} F_x \\ F_y \end{Bmatrix} = K_d \begin{Bmatrix} U_x \\ U_y \end{Bmatrix} + (\sigma_{YL(T)} A_L) \begin{Bmatrix} Z_x \\ Z_y \end{Bmatrix} \tag{1}$$

2

Whereas in the case of friction pendulum bearings its hysteretic behaviour is represented as follows:

$$\begin{Bmatrix} F_x \\ F_y \end{Bmatrix} = -P \begin{Bmatrix} \dfrac{u_x}{R_x} \\ \dfrac{u_y}{R_y} \end{Bmatrix} - P \begin{Bmatrix} \mu_x Z_x \\ \mu_y Z_y \end{Bmatrix} \tag{2}$$

Both hysteretic models depend on two dimensionless hysteretic variables, $Z_x$ and $Z_y$, as proposed by Park et al. [4] for coupled bidirectional systems. These variables are restricted to have the following range

$$\sqrt{Z_x^2 + Z_y^2} \le 1 \tag{3}$$

At the same time, these dimensionless variables obeys the following nonlinear differential equation

$$Y \begin{Bmatrix} Z_x \\ Z_y \end{Bmatrix} = \left( A[I] - \begin{bmatrix} Z_x^2(\gamma Sign(\dot{U}_x Z_x) + \beta) & Z_x Z_y(\gamma Sign(\dot{U}_y Z_y) + \beta) \\ Z_x Z_y(\gamma Sign(\dot{U}_x Z_x) + \beta) & Z_y^2(\gamma Sign(\dot{U}_y Z_y) + \beta) \end{bmatrix} \right) \begin{Bmatrix} \dot{U}_x \\ \dot{U}_y \end{Bmatrix} \tag{4}$$

The constants A, β and γ, called evolution constants, control the shape of the hysteretic loop.

With the aim of gaining a fully comprehensive understanding of the hysteretic behaviour of LRBs and TFPBs, a MATLAB code was developed to simulate benchmark hysteretic results. After solving the nonlinear differential equations of motion using the developed code, the results were replicated using a commercial software like SAP2000 [5].

A numerical model developed by Kalpakidis et al. [6] considers the strength degradation of LRBs due to lead-core heating effects. In this model, the yield stress of lead core is not constant and decreases with the number of hysteretic cycles. As a result, the characteristic strength of LRBs depends on the temperature variation in the lead, which is a function of the time.

Some of the results obtained by Kalpadikis et al. [7] were replicated. The seismic records adopted in this analysis were the Tabas earthquake in 1995 (Iran), Kobe earthquake in 1995 (Japan) and the Duzce earthquake in 1978 (Turkey).

The results obtained with the Kalpakidis model [6] were compared utilizing a bilinear hysteretic model with upper and lower bound values of characteristic strength. The obtained results are shown in Fig.2 and Fig.3.
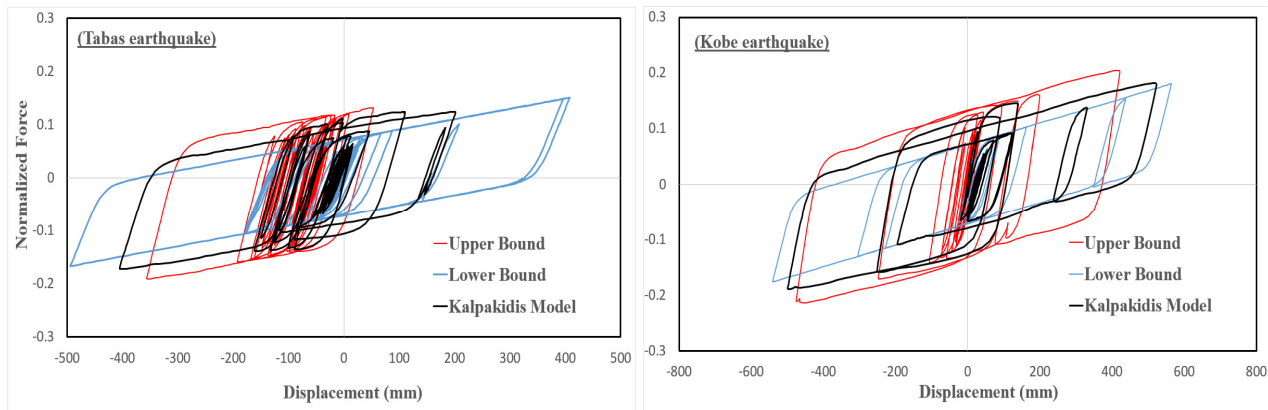


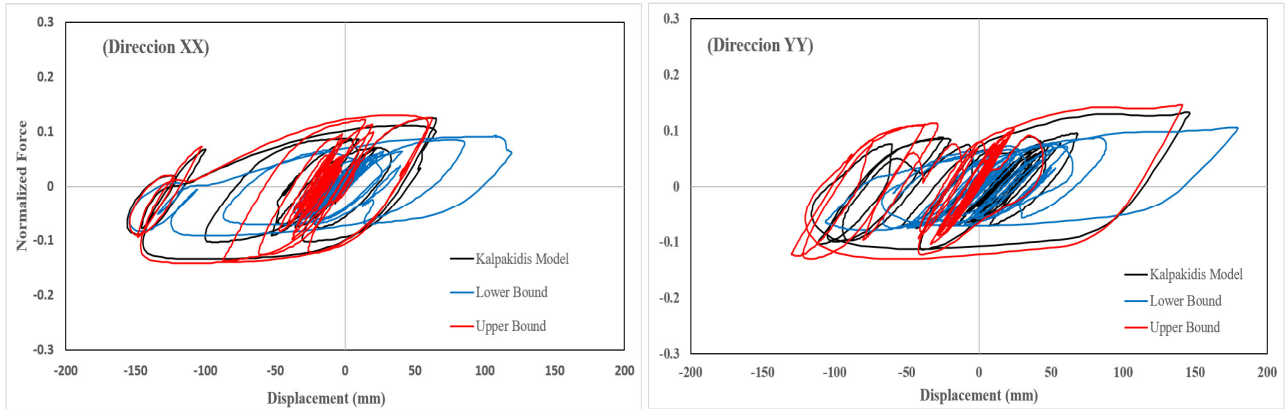Fig. 2 – Obtained hysteresis loops for LRB (Tabas and Kobe earthquake)

3

Fig. 3 – Obtained hysteresis loops for LRB (Duzce earthquake)

In the case of the friction pendulum isolators, friction coefficients are set for a fast sliding, $\mu_{max}$, and slow sliding, $\mu_{min}$, as well as a speed change parameter, r, describing the transition between the two limits. The values adopted in the previous parameter, r, and the relationship between the friction coefficients are related to the experimental results obtained by Nagarajaiah et al. [8]

$$\mu_x = \mu_{xmax} - (\mu_{xmax} - \mu_{xmin})e^{-r\dot{U}} \tag{5}$$

$$\mu_x = \mu_{xmax} - (\mu_{xmax} - \mu_{xmin})e^{-r\dot{U}} \tag{6}$$

According to Constantinou et al. (2011) [9], there are two simplified ways to represent the hysteric behaviour of TFPBs using Single Friction Pendulum Bearings (SFPBs). The first way uses two SFPB elements in parallel which are attached to the same nodes, whereas the second uses three SFPB elements placed between the nodes in series.

For the TFPB isolators, the experimental tests carried out by Becker [10] were taken as benchmark results. The seismic records of Northridge Earthquake in 1994 (USA) and Tabas Earthquake in 1978 (Iran) were adopted to replicate the hysteretic behaviour observed in the dynamic test.

In the development of the numerical model, the TFP isolator was modelled using the serial model, which consist of three SFPB elements [11]. The obtained results are showed in Fig.4 and Fig.5.
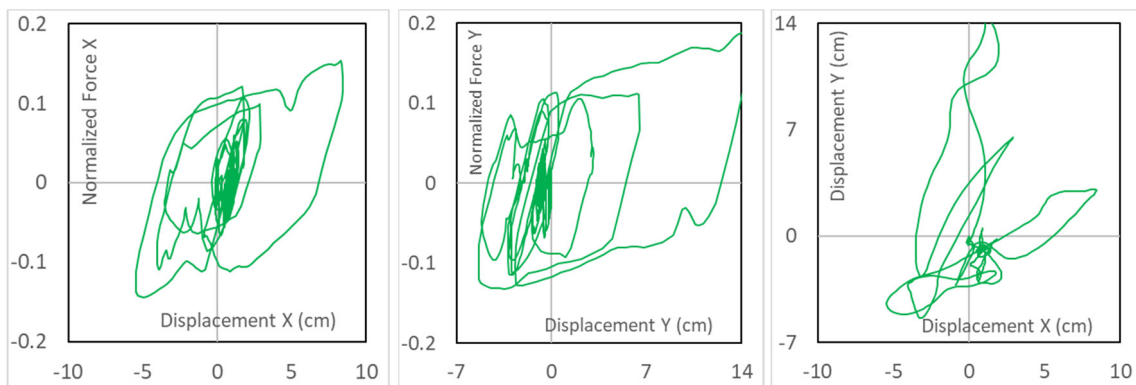


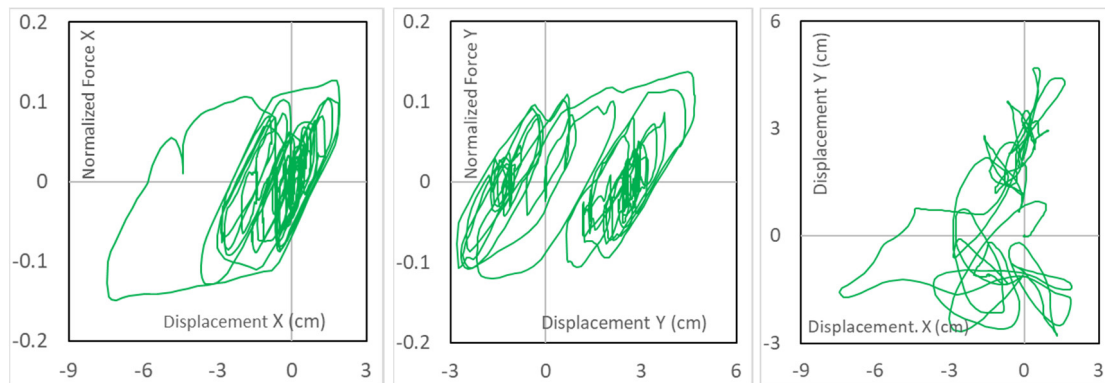Fig. 4 – Obtained hysteresis loops for TFPB (Northridge Earthquake)

Fig. 5 – Obtained hysteresis loops for TFPB (Tabas Earthquake)

## 3. Adopted Design of the Isolators

In order to perform a better comparative assessment of the seismic performance of the both types of isolators, the conventional bearings of an existing three-span continuous composite highway bridge were redesigned. In this redesign, two schemes of the bridge were generated, one using a LRB layout and other using a TFPB layout. These isolators were designed according to the criteria set by Eröz and DesRoches [2] with the aim of comparing the unique effects of each type of isolator. This adopted criteria states that:

- The isolated periods should be similar for both isolation systems.
- Similar yield force values and post-yield stiffness
- Uniform bearing sizes used in each scheme

In this study, it was established that the isolated period of each bridge is approximately 3 seconds. During the isolation design, the unimodal analysis method [12] was performed. Each isolated bridge was designed considering two isolators under each support of the deck (piers and abutments). The resulting dimensions of the isolators are summarized in Table 1 and Table 2.

Table 1 – Isolator properties LRB

|  | Pier | Abutment |
|---|---|---|
| Isolator diameter (m) | 0.80 | 0.80 |
| Lead core diameter (m) | 0.14 | 0.14 |
| Total thickness rubber (m) | 0.30 | 0.30 |
| Lead effective yield stress (MPa) | 10 | 10 |
| Shear modulus of rubber (MPa) | 0.414 | 0.414 |

Table 2 – Isolator properties TFPB

|  | Pier | Abutment |
|---|---|---|
| Radius of curvature 1, 4 (m) | 2.24 | 2.24 |
| Radius of curvature 2, 3 (m) | 0.41 | 0.41 |
| Distance d1, d4 (m) | 0.28 | 0.28 |
| Distance d2, d3 (m) | 0.05 | 0.05 |
| Friction coefficient $\mu1, \mu4$ | 0.0685 | 0.0685 |
| Friction coefficient $\mu2, \mu3$ | 0.0444 | 0.0444 |

5

2g-0160

## 4. Numerical modelling of the Bridge

In the development of the numerical model, only beam-column elements and bearing elements were considered (Fig.6). The behaviour of the superstructure and substructure was assumed to remain within the linear-elastic range, as a consequence of the isolation design considered. The effective flexural stiffness of the column elements was obtained through a moment-curvature analysis of the cross section. In contrast to the beam-column elements, the isolation bearings are the unique elements that considered a hysteretic behaviour.
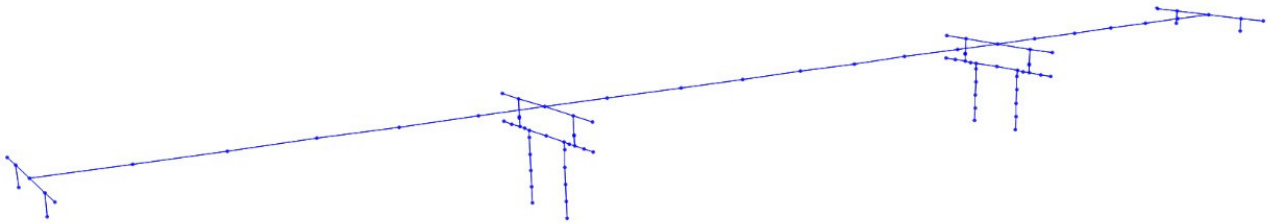


Fig. 6 – Three-dimensional modelling of the bridge

The continuous deck of the bridge consists of three spans of 35 m, 50 m and 35 m, respectively. The deck is made up of five steel girders of type I, a reinforced concrete slab, and steel cross-frame diaphragms as is shown in Fig.7. The bridge substructure consists of two intermediate piers which are made up of two circular columns (Fig.8) which are 120 $cm$ in diameter and 6.10 $m$ in height. The calculated total weight of the superstructure and substructure are $W_{sup} = 16760\ kN$ and $W_{sub} = 1093\ kN$, respectively [13].
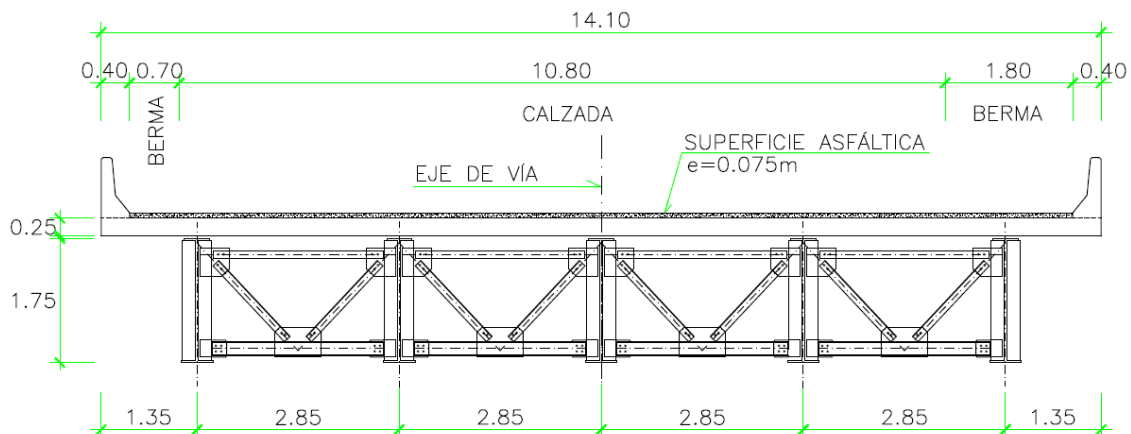


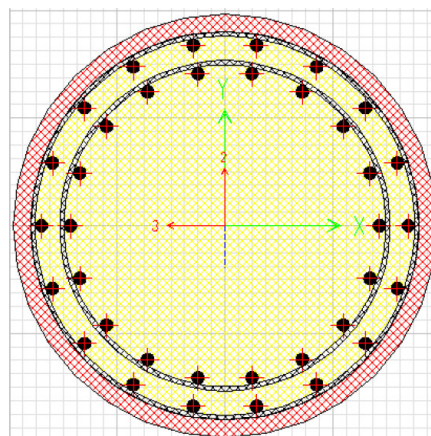Fig. 7 – Cross section of the superstructure



Fig. 8 – Cross section of the column in the substructure

6

The nonlinear time-history analysis was performed according to the guidelines of ASCE / SEI 7-16 [14]. These guidelines states that the seismic analysis and design must consider only the Maximum Considered Earthquake (MCE). This earthquake has a 2 percent probability of being exceeded in a 50-year period, which means a recurrence period of 2500 years. Seven pairs of seismic records (Table 3) were used in the dynamic analysis. These records were scaled [14] to the spectrum of accelerations related to the MCE earthquake for the City of Lima in Peru, as it is shown in the Fig.9.
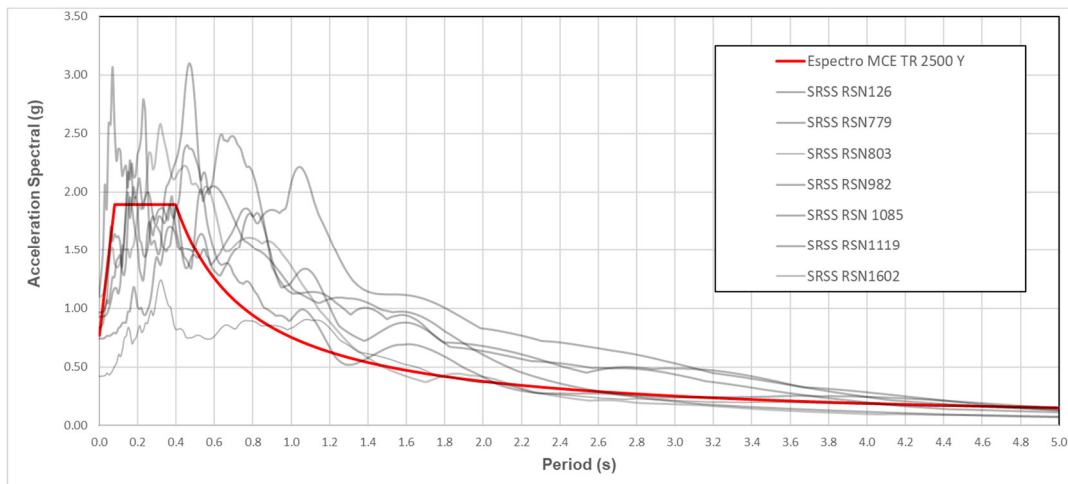


Fig. 9 – SRSS elastic response spectrum of the 7 pairs seismic records and the MCE acceleration spectrum

Table 3 – Seven pairs of ground motions used in the seismic analysis

| Code PEER # | Name of the accelerogram | Station | $M_W$ | $R_{rup}$ (km) |
|---|---|---|---|---|
| RSN126 | 1976 Gazli USRR | Karakyr | 6.8 | 5.46 |
| RSN779 | 1989 Loma Prieta | LGPC | 6.93 | 3.88 |
| RSN803 | 1989 Loma Prieta | Saratoga, W. Valley Coll. | 6.93 | 9.31 |
| RSN982 | 1994 Northridge | Jensen Filter Plant | 6.69 | 5.43 |
| RSN1085 | 1994 Northridge | Sylmar, Coverter Sta. East | 6.69 | 5.19 |
| RSN1119 | 1995 Kobe Japan | Takarazuka | 6.90 | 3.00 |
| RSN1602 | 1999 Duzce Turkey | Bolu | 7.14 | 12.4 |

## 4. Numerical Results

For the time history analysis, the upper and lower limits were considered by means of property modification factors. Through this way, the maximum absolute values in terms of displacement and shear forces were obtained. The Table 4 shows the lambda factors to be used in the analysis. This values were taken from the work developed by McVitti and Constantinou [15].

Table 4 – Property modification factors for both isolators

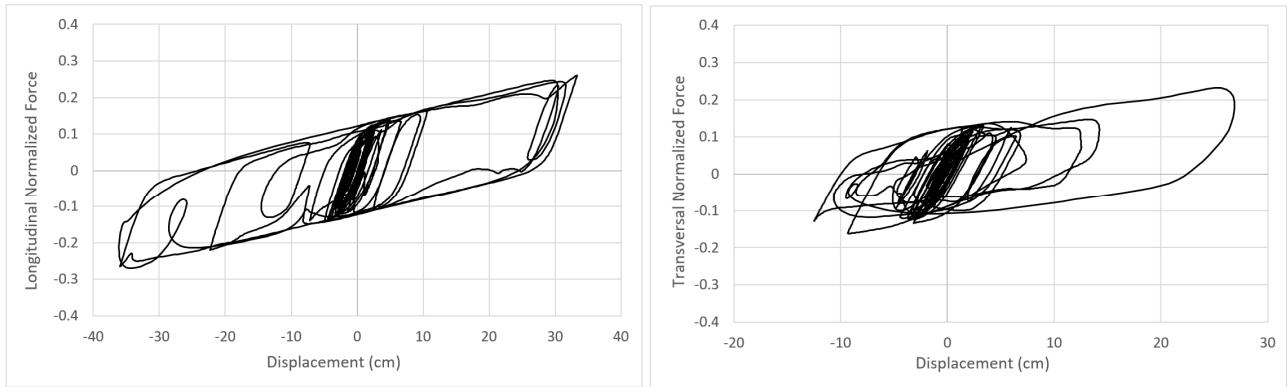| | Lead Rubber | | Friction Pendulum | |
|---|---|---|---|---|
| | G | $\sigma_L$ | $\mu_{1-4}$ | $\mu_{2-3}$ |
| $\lambda_{max}$ | 1.83 | 1.84 | 2.12 | 2.12 |
| $\lambda_{min}$ | 0.76 | 0.76 | 0.6 | 0.6 |

7

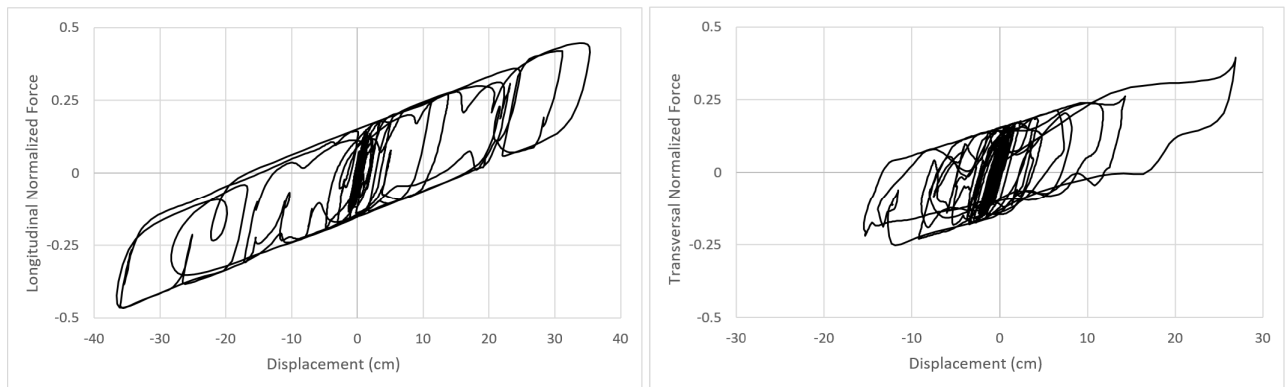Fig. 10 – Obtained Hysteresis loops for LRB at abutments (Duzce earthquake)



Fig. 11 – Obtained Hysteresis loops for TFPB at abutments (Duzce earthquake)

The seismic demands of the isolators and columns along the same transverse axis were the same. Therefore, the obtained results are presented for one of the isolators, at the top of pier or abutment, and one of the columns, at the piers. From the nonlinear time-history analysis, the hysteretic behaviour of each isolator layout was captured under the horizontal ground motions. Some of these results are shown in fig.10 and fig. 11.
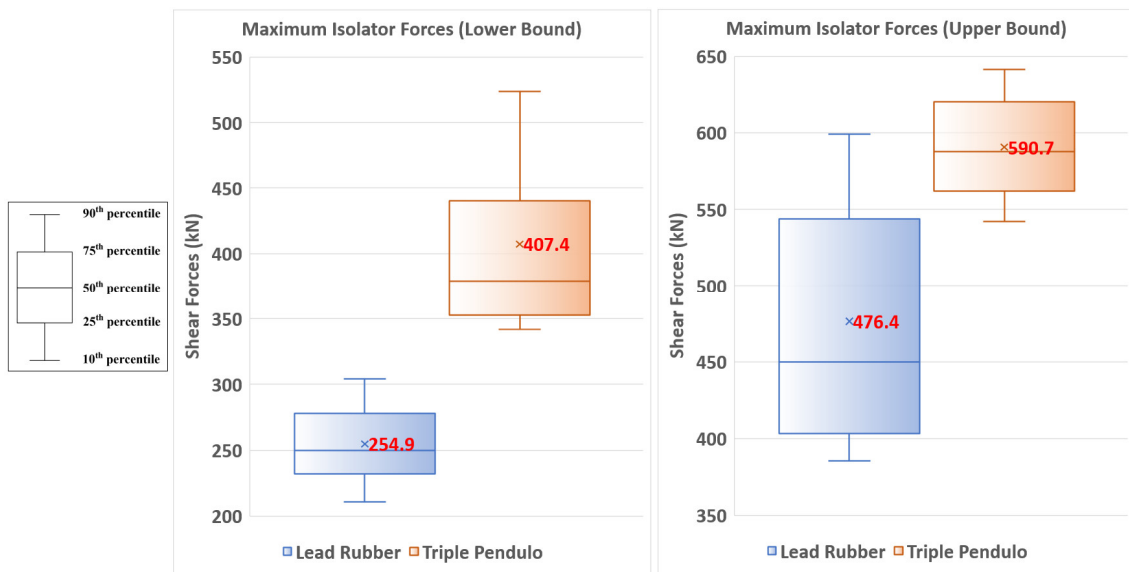


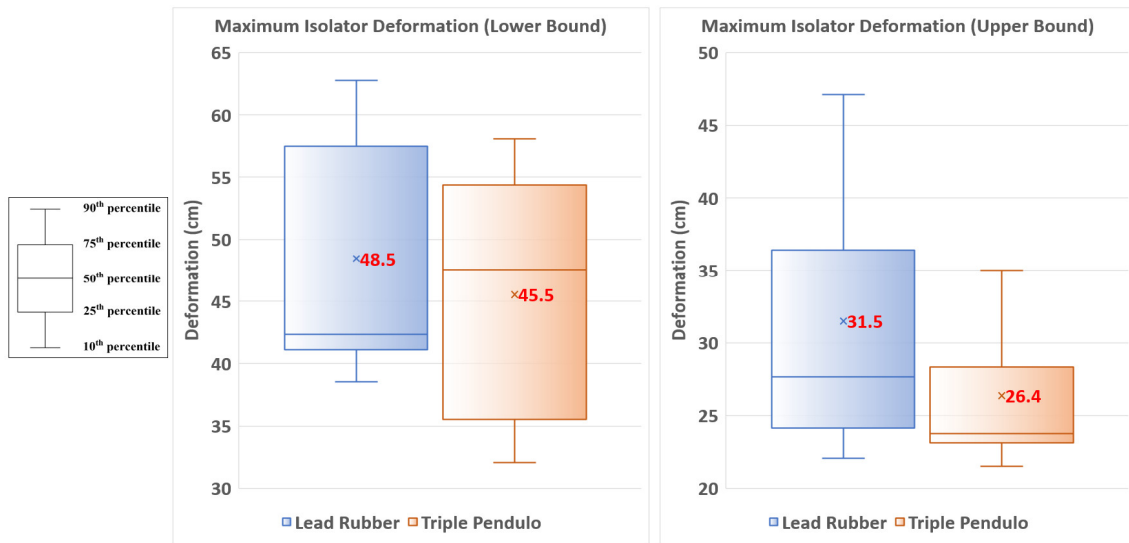Fig. 12 – Maximum isolator forces (MIF) on the top of the pier

8

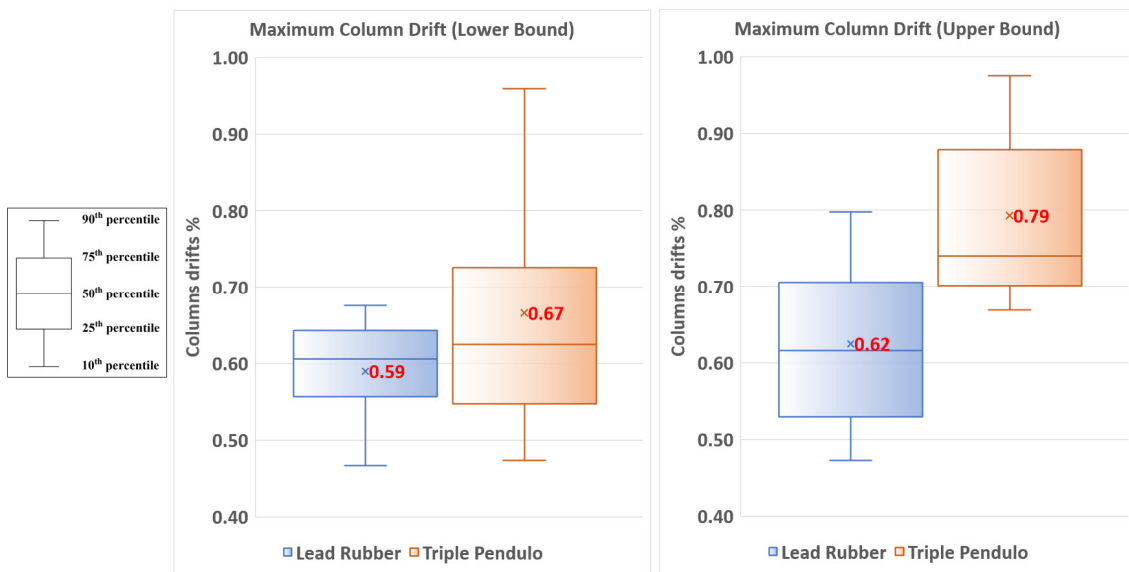Fig. 13 – Maximum isolator deformations (MID) on top of the abutments



Fig. 14 – Maximum columns drifts in the piers

The maximum absolute values measured in the isolators and columns are: (1) the maximum shear force in the isolator (MIF), (2) the maximum displacement in the isolator (MID), and (3) the maximum distortion in the columns, $d_{max}$. These maximum absolute values are shown in Fig. 12, Fig. 13 and Fig. 14. In these figures the mean values, and different cumulative percentiles of the seismic demands are plotted.

## 5. Conclusions

- Despite having similar periods, the analysis of the isolated bridges shows that there are differences in the forces and displacements experienced by the isolators and the column elements.
- The obtained results indicate that the lower bound analysis generates higher displacements in the LRB scheme. In this case, the resulting displacement in the LRB isolators was 7% higher than the obtained in the TFPB isolator.

9

2g-0160

- In the case of the upper bound analysis, the highest shear forces in the isolators and the highest distortions in the columns were obtained. From this analysis, the induced forces in the LRBs were 19% lower than the acting forces in the TFPBs. As a result, the TFPBs induce higher distortions in the columns than the LRB scheme. These obtained values were 0.62% and 0.79%, respectively.
- From the results, it is observed that the LRB layout induces a more uniform distribution of forces along the bridge compared to the TFPB layout. In the case of the TFPBs, its rigidity and then the induced shear forces depends on the tributary mass supported by the isolators.

## 6. References

[1] Priestley M. J. N., Seible F. and Calvi G. M. (1996). Seismic Design and Retrofit of Bridges. *John Wiley and Sons, New York*

[2] Eroz M. and DesRoches R. (2014): A Comparative Assessment of Sliding and Elastomeric Seismic Isolation in a Typical Multi-Span Bridge. *J. Earthq. Eng.*, vol 17, n. 5, p. 637-657.

[3] Wen Y. (1976). Method for random vibration of hysteretic system. *Journal of the engineering mechanics division. Abril . 102 (EM2):249-26*

[4] Park Y. J., Wen Y. K. and Ang A. H-S. (1986). Random Vibration of Hysteretic Systems Under Bi-Directional Ground Motions. *Earthquake Engineering and Structural Dynamics, Vol. 14, pp. 543-557.*

[5] CSI (2017), CSI Analysis Reference Manual for SAP2000, ETABS, SAFE and CSiBridge. *Computers and Structures, Inc. Berkeley, USA*

[6] Kalpakidis I., and Constantinou M. (2008). Effects of Heating and Load History on the Behavior of Lead-Rubber Bearings. *MCEER Earthquake Engineering to Extreme Events*, New York, USA.

[7] Kalpakidis I., Constantinou M. and Whittaker S. (2010). Modeling strength degradation in lead–rubber bearings under earthquake shaking. *Earthquake Engineering and Structural Dynamics.*

[8] Nagarajaiah S, Reinhorn A.M., and Constantinou, M.C. (1989). Nonlinear Dynamic Analysis of Three-dimensional Base Isolated Structures (3D-BASIS). *Report NCEER-89-0019, National Center for Earthquake Engineering Research, State University of New York, Buffalo, NY.*

[9] Constantinou M., Kalpakidis I., Filiatrault A., and Ecker Lay R. (2011). LRFD-Based Analysis and Design Procedures for Bridge Bearings and Seismic Isolators. *MCEER Earthquake Engineering to Extreme Events*, New York, USA.

[10] Becker T. C. (2011). Advanced Modeling of the Performance of Structures Supported on Triple Friction Pendulum Bearings. *University of California, Berkeley*

[11] Fenz D. and Constantinou M. (2008). Modeling Triple Friction Pendulum Bearings for Response-History Analysis. *Earthquake Engineering Research Institute*

[12] AASHTO. (2014). Guide Specifications for Seismic Isolation Design. *4th Edition. Washington DC, USA: American Association of Highway and Transportation Officials.*

[13] Melchor C. (2016). Influencia de los Apoyos Elastoméricos en la Respuesta Sísmica de Puentes. *Universidad Nacional de Ingenieria, Lima, Peru.*

[14] American Society of Civil Engineers (2016). Minimum Design Loads and Associated Criteria for Buildings and Other Structures. *Standard ASCE/ SEI 7-16*

[15] McVitty W., and Constantinou M. (2015). Property Modification Factors for Seismic Isolators: Design Guidance for Buildings. *MCEER Earthquake Engineering to Extreme Events*, New York, USA.

10